STUDIA UBB CHEMIA, LXI, 1, 2016 (p. 199-212)
(RECOMMENDED CITATION)

Dedicated to Professor Mircea Diudea on the Occasion of His 65th Anniversary

THE AGGREGATION BEHAVIOR OF AN A_3B FREE BASE PORPHYRIN AND ITS APPLICATION AS CHROMIUM(III)-SELECTIVE MEMBRANE SENSOR

BOGDAN-OVIDIU ŢĂRANU[a], DANA VLASCICI[b], IULIANA SEBARCHIEVICI[a], EUGENIA FĂGĂDAR-COSMA[c,*]

ABSTRACT. A polyvinyl chloride membrane chromium(III)-selective electrode based on a synthesized A_3B free base porphyrin, namely 5-(4-pyridyl)-10,15, 20-tris(phenoxy-phenyl)porphyrin, as membrane carrier was formulated and evaluated. The electrode exhibits a near-Nernstian response over the chromium(III) concentration range of $3x10^{-5}$ ÷ $1x10^{-1}$ M and shows good selectivity with respect to a wide range of cations. The aggregation behavior of the porphyrin macrocycle was investigated using TEM and STEM analytic techniques and revealed the formation of different shapes of nanostructures. Electron tomography was also employed in the study of the porphyrin aggregates.

Keywords: *membrane carrier, A_3B porphyrin, aggregation behavior, electron tomography*

INTRODUCTION

The vast majority of metals and metallic complexes with industrial use present some type of ecological hazard. Of these, chromium is a pollutant of considerable concern, as it is highly toxic and finds widespread use in industrial fields, such as: leather tanning, electroplating, steel manufacturing, metal finishing,

[a] *National Institute of Research-Development for Electrochemistry and Condensed Matter Timisoara, Dr. Aurel Paunescu Podeanu str., no. 144, 300569 Timisoara, Romania*
[b] *Faculty of Chemistry-Biology-Geography, West University of Timisoara, Pestalozzi str., no. 16, 300115 Timisoara, Romania*
[c] *Institute of Chemistry Timisoara of Romanian Academy, Mihai Viteazul Ave., no. 24, 300223 Timisoara, Romania*
** Corresponding Author: efagadar@yahoo.com*

alloy manufacturing, wood treatment and oxidative dyeing. It is also an essential element in human nutrition, but exposure to high concentrations leads to irritation of skin and mucous membranes, ulcerations, liver and kidney damage, as well as lung cancer [1]. Chromium adds desirable properties in alloys with iron, nickel, and other metals, such as the hardness and corrosion resistance of chrome steel [2]. It can exist in trivalent and hexavalent states [3] and both forms have been found in industrial and environmental situations [1]. According to Sharma *et al.* [4] more than 80% of tanneries in South Asian and African countries engage in the leather tanning practice where the leather takes 50 to 60% chromium while the rest is discharged as waste. In South Asian tanneries about 50,000 metric tons of chromium salt is discharged into wastewater streams annually, causing environmental pollution.

Therefore, from an environmental point of view, there is a strong need to determine chromium ions using reliable methods. One such method is the potentiometric determination by ion-selective electrodes (ISEs) and it offers several advantages: it doesn't require any specialized equipment or sample pretreatment, it allows for a fast analysis, it's a low cost and nondestructive method, it can detect the target ion in a wide dynamic range and with fairly good selectivity.

A literature survey reveals that several chromium(III) selective ISEs have been reported in the last decades. These sensors were obtained using a variety of compounds as ionophores. In 1980 Masuda *et al.* reported for the first time on chromium(III) by studying the response of a PVC based electrode wire coated with Cr(III) and incorporating Aliquat 336S tetrakis-(thiocyanato)chromate(III) ion pair [5]. The electrode exhibited a Nernstian slope of 58 mV/pCr over the $10^{-5} \div 10^{-2}$ concentration range. In 1996 a PVC membrane based Cr(VI)-selective electrode incorporating nickel tris(1,10-batho-phenanthroline)hydrogen chromate as ionophore was developed. The sensor was used for sequential determination of Cr(VI) and Cr(III) by direct monitoring of Cr(VI) followed by oxidation of Cr(III) and measurement of the total chromium [6]. Another PVC based Cr(III)-selective electrode was reported by Singh *et al.* [7]. The ionophore for this sensor was 3,10-*c*-*meso*-3,5,7,7,10,12,14,14-octamethyl-1,4,8,11-tetraazacyclotetra-decane diperchlorate and the best results obtained by varying the composition of the membranes indicated that the Cr(III)-selective electrode can exhibit a Nernstian slope of 20 mV/decade of activity over the $1.77 \times 10^{-6} \div 10^{-1}$ M concentration range. Dimethylaminoazobenzene was also incorporated as membrane carrier in a PVC membrane during the development of a Cr(III)-selective electrode [8]. The sensor revealed a Nernstian response with a slope of 19.5 mV/decade over the $1.66 \times 10^{-6} \div 10^{-2}$ M concentration range. The construction of solid-contact Cr(III)-selective film electrodes based on

titanium diselenide and titanium ditelluride intercalated with chromium was also reported [9]. The electrode containing titanium diselenide proved to be a sensor for the determination of Cr(III) over the $5x10^{-5} \div 10^{0}$ M concentration range. A PVC membrane based ISE using glyoxal bis(2-hydroxyanil) as ionophore was developed and studied as sensor for the determination of Cr(III) cations [10]. The electrode exhibited a Nernstian slope of 19.8 mV/decade over the $3x10^{-6} \div 10^{-2}$ M concentration range with a detection limit of $6.3x10^{-7}$ M. In 2004 Sil *et al.* [11] tested tetraazacyclotetradecane, tetratosyltetraaza 12C4 and tritosyltriaza 9C3 as ionophores in PVC based coated wire Cr(III)-selective electrodes. The best performance was observed for the electrode incorporating tetratosyltetraaza 12C4 dibutyl phthalate plasticizer and PVC in the 5:60:35 (w/w) ratio. It exhibited a Nernstian slope of 20 mV/decade over the $10^{-7} \div 10^{-1}$ M concentration range with a detection limit of $6x10^{-8}$ M. The ionophore 2,10-dimethyl-4,12-diphenyl-1,5,9,13-tetraazacyclohexadeca-1,4,9,12-tetraene was incorporated in a polystyrene-based membrane and the selectivity of the resulting electrode was investigated in solutions containing Cr(III) ions. The best sensor had a Nernstian slope of 19.5 mV/decade over the $1.6x10^{-6} \div 10^{-1}$ M concentration range [12]. In another study, a Cr(III)-specific potentiometric sensor was developed using a synthesized chelating resin, namely: Aurin tricarboxylic acid modified silica. A PVC membrane electrode of the modified silica was developed and evaluated as sensor for Cr(III) cations. It exhibited a Nernstian slope of 19 mV/decade of concentration over the $7\times10^{-6} \div 10^{-1}$ M concentration range [4]. Ganjali *et al.* used *N*-(1-thien-2-ylethylidene)benzene-1,2-diamine as ionophore in PVC membrane based electrodes that were subsequently tested as sensors for Cr(III) ions. The best sensor obtained after changing the ratio between the membrane components exhibited a Nernstian slope of 19.9 mV/decade over the $10^{-6} \div 10^{-1}$ M concentration range with a detection limit of 7×10^{-7} M [13]. In another report, a Cr(III)-selective electrode based on tri-*o*-thymotide in PVC matrix was manufactured and studied. The best sensor, obtained after changing the ratio between membrane components, showed a Nernstian slope of 20 mV/decade of activity over the $4\times10^{-6} \div 10^{-1}$ M concentration range with a detection limit of 2×10^{-7} M [14]. A PVC based Cr(III)-selective electrode incorporating di(benzylamino)glyoxime as ionophore was also studied. The sensor exhibited a Nernstian slope of 20.3 mV/decade over the $10^{-6} \div 10^{-1}$ M concentration range with a detection limit of 2×10^{-7} [15]. Zamani *et al.* [16,3,17,18] reported the development and evaluation of several Cr(III)-selective electrodes based on different compounds as carriers in PVC membranes: 4-amino-3-hydrazino-6-methyl-1,2,4-triazin-5-one;1,3-diamino-2-hydroxypropane-N,N,N', N'-tetraacetic acid; 5-amino-1-phenyl-1H-pyrazole-4-carboxamide and diethyl 2-phthalimidomalonate.

The reports published in the scientific literature outline the variety of membrane carriers used to manufacture Cr(III)-selective potentiometric sensors. However, to the best of our knowledge no Cr(III) ISE using a porphyrin as ionophore was ever developed. Porphyrins are macrocyclic compounds with properties that make them suitable to be used as membrane carriers in PVC membrane based potentiometric sensors [19-21]. Therefore, in the present work, a PVC membrane chromium(III)-selective electrode based on a synthesized A_3B free base porphyrin, namely 5-(4-pyridyl)-10,15,20-tris(phenoxy-phenyl)porphyrin, as ionophore was formulated and evaluated.

The aggregation behavior of the A_3B porphyrin from tetrahydrofuran solution was investigated using Transmission Electron Microscopy (TEM) and Electron Tomography. TEM is a valuable technique for studying materials at the submicron- and nanoscale [22-24], while electron tomography can be used to create 3D reconstructions from 2D projection images [25]. In the latter case, the projections are acquired at different tilt angles of the specimen, they undergo a process of alignment and the resulted tilt-series is used as input for a mathematical algorithm, such as Weighted Back-Projection (WBP) and Simultaneous Iterative Reconstruction Technique (SIRT) [26], leading to a 3D reconstruction.

RESULTS AND DISCUSSION

Investigation of porphyrin samples using electron microscopy. TEM and STEM images obtained for the porphyrin samples in TEM Bright Field (BF) and STEM High-Angle Annular Dark Field (HAADF) modes are shown in Figures 1 and 2, respectively.

When the porphyrin aggregation behavior was investigated using electron microscopy, different types of structures were evidenced. Most aggregates resembled islands with circular and elliptical shapes (Figures 1a and 2a). Measurements performed on the circular formations revealed their diameters to range from the microscale all the way to the nanoscale (as small as 71.7 nm). These islands bear resemblance to other porphyrin structures reported in the literature as having their macrocycles oriented nearly parallel to the surface of the support [27]. The two types of structures further organize together into collections of aggregates bearing ovoidal shapes.

A few areas from the TEM grids also showed the presence of spherical aggregates (Figures 1b, 2b and 2c). The diameters of these spheres ranged from the submicron to the nanoscale. These structures can coexist with the other types of aggregates (Figures 2b and 2c) and even join with other spheres to form bundles (Figure 2c).

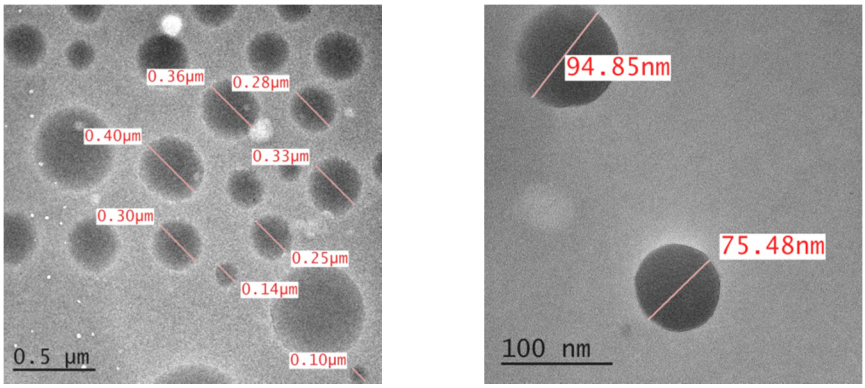

a b

Figure 1. BF TEM images recorded for the porphyrin sample. a) Circular aggregates; b) Spherical aggregates

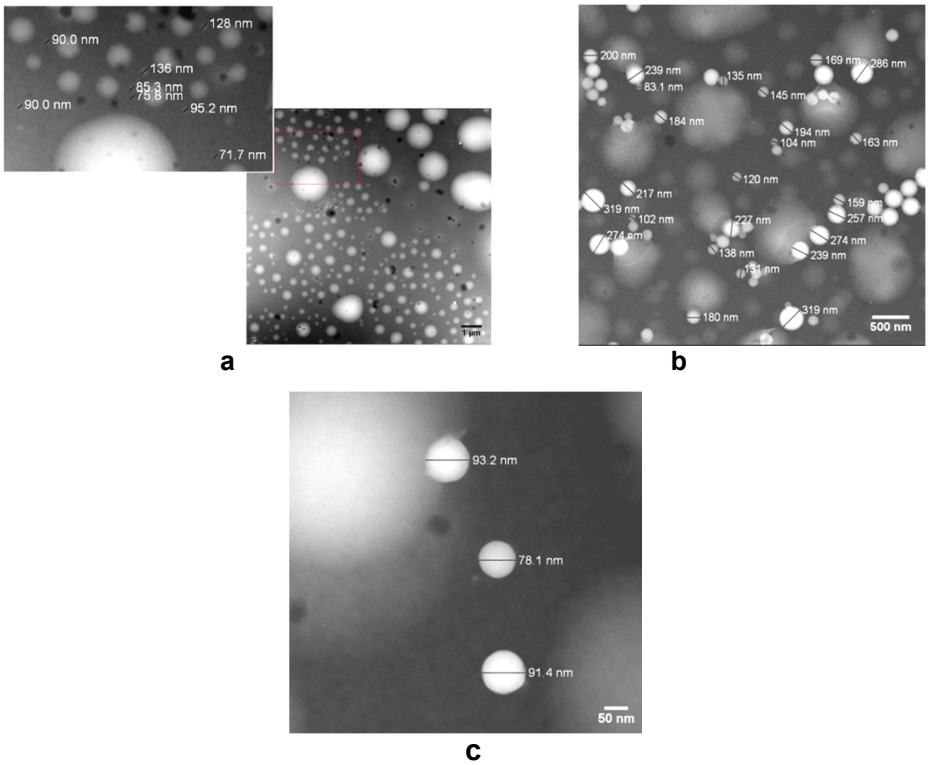

a b c

Figure 2. HAADF STEM images recorded for the porphyrin sample. a) Circular and elliptical aggregates. Inset showing enlarged area; b and c) Spherical aggregates with ovoidal aggregates in the background

Electron tomography of porphyrin aggregates. Figure 3a shows the porphyrin aggregate selected for 3D reconstruction using HAADF STEM Tomography and the reconstructed volume. The tilt series was recorded by setting the Max negative and positive tilts at -59º and 63º, respectively and the Low tilt step at 1º. The 3D reconstruction of the aggregate appears as a spheroid and it shows a slight elongation due to missing wedge artefacts generated by the limited spacing in between the pole pieces of the objective lens in the microscope column and by the tilt range selected for the holder during the acquisition. Even holders with tilt ranges higher than ± 80º can cause an unsampled region in frequency space, referred to as the missing wedge region [28].

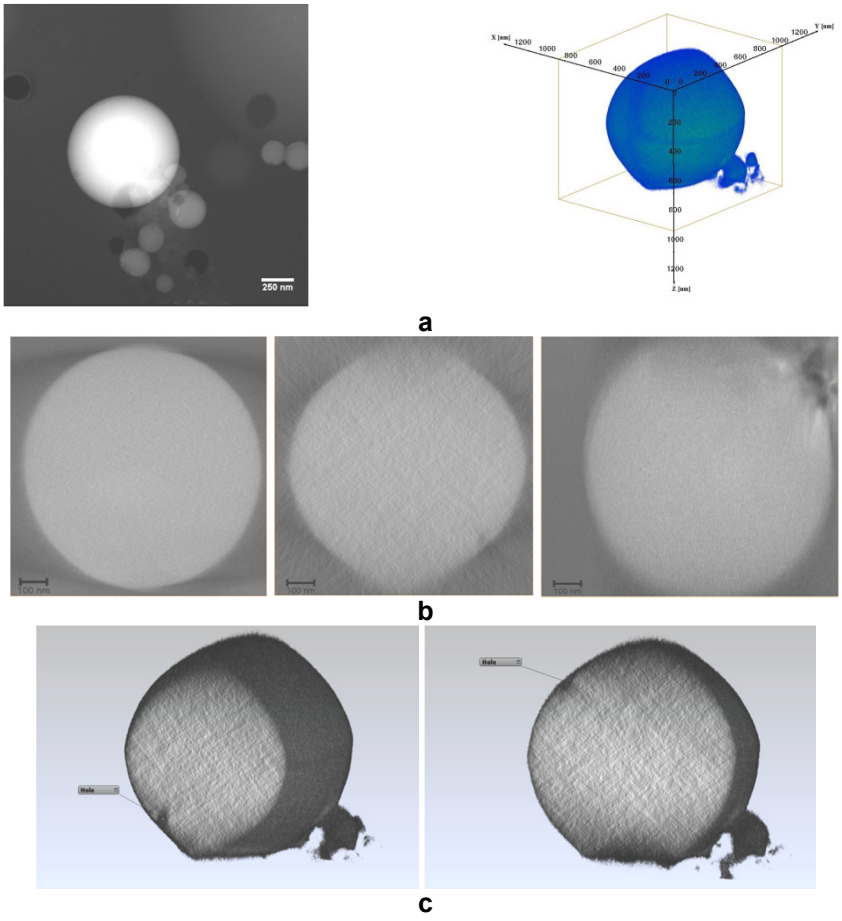

Figure 3. a) STEM image at 0º and the reconstructed volume (955 x 1,097 x 957 nm^3) of porphyrin aggregate; b) XY, XZ and YZ orthoslices; c) sections through the 3D volume

Figure 3b shows the XY, XZ and YZ orthogonal slices half way through the reconstructed volume and together with Figure 3c reveals the interior of the object to be almost entirely filled. The only exceptions are a couple of holes located near the edge of the aggregate, with dimensions in the nanoscale.

Detection studies. 5-(4-pyridyl)-10,15,20-tris(phenoxy-phenyl)porphyrin was used as a ionophore for the obtaining of four potentiometric sensors different due to their composition and plasticizers used, which are presented in Table 1. The sensors were tested for a number of monovalent, divalent and trivalent cations and appear to be chromium-selective, having different working concentration ranges and different slope values (Table 1).

Table 1. Composition of the membranes and response characteristics of the sensors

Sensor	% Composition (w/w) of the membranes					Working concentration range (M)	Slope (mV/decade)
	Ionophore	PVC	NPOE	DOS	DOP		
1	1	33	66			$1x10^{-1} \div 3x10^{-5}$	18.11
2	1	33		66		$1x10^{-2} \div 1x10^{-5}$	21.91
3	1	33			66	$1x10^{-1} \div 1x10^{-6}$	42.88
4	1.4	32.87	65.73			$1x10^{-1} \div 1x10^{-4}$	17.92

According to the results presented in Table 1, a bigger amount of porphyrin does not improve the potentiometric answer of the sensor. In the terms of working concentration range, the best results were obtained for the sensor having dioctylphtalate as plasticizer, but in this case, the slope was double Nernstian, so the sensor is not useful. By meaning of both, working concentration range and slope, the optimum composition was obtained using *o*-nitrophenyloctylether as plasticizer with a slope of 18.11 mV/decade of concentration and working from $1x10^{-1} \div 3x10^{-5}$ M.

The potentiometric answer of the optimum composition sensor to all the cations used is presented in Figure 4 and the potentiometric response toward chromium(III) is presented in Figure 5.

The practical response time of the sensor to reach the equilibrium potential was obtained after successive immersion of the electrode in a series of chromium(III) solutions, each having a 10-fold difference in concentration. The response time was about 10 s as the concentration of chromium (III) varies from 10^{-3} to 10^{-2} M. The detection limit of the electrode having the optimum composition, established at the point of intersection of the extrapolated linear mid-range and final low concentration level segments of the calibration plot was $9x10^{-6}$ M.

The sensor was used for a period of 50 days, without significant changes in the values of the slope and no change in the working concentration range.

One important characteristic of a potentiometric sensor is the interference of other ions in the potentiometric answer of the main one. The values of the selectivity coefficients, calculated by separate solution method are presented in Table 2.

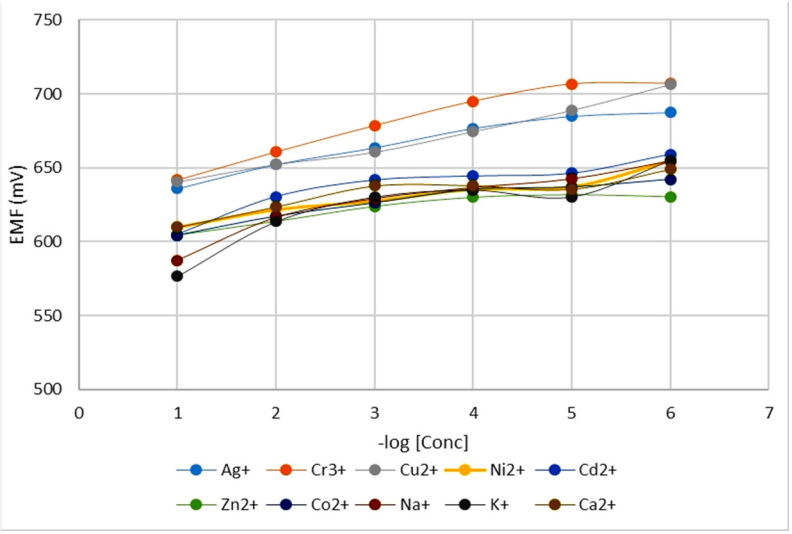

Figure 4. Potentiometric response of the sensor having the optimum composition of the membrane toward different metal ions.

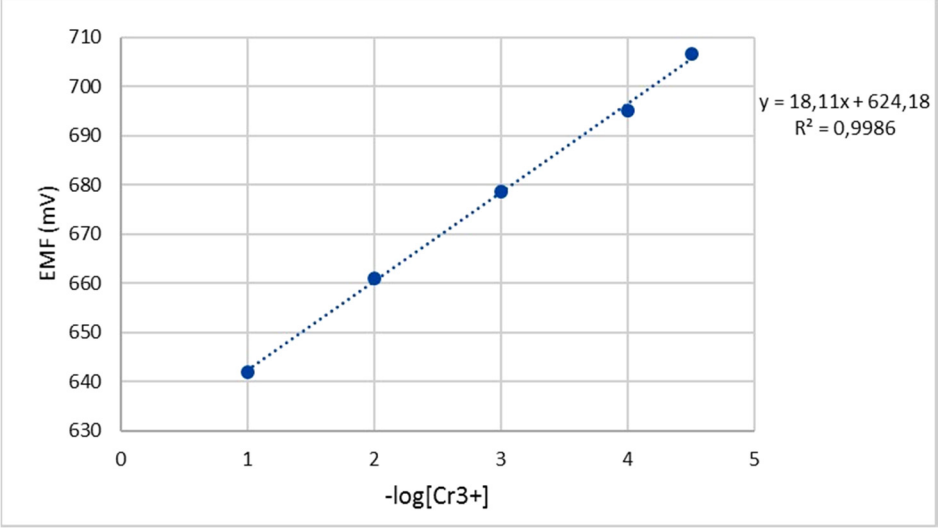

Figure 5. Potentiometric response to chromium of the optimum composition sensor

Table 2. The values of the selectivity coefficients

Interfering cation	$\log K_{Cr,Y}^{pot}$
Ag^+	-4.44
Cu^{2+}	-1.44
Ni^{2+}	-2.99
Cd^{2+}	-2.54
Zn^{2+}	-3.40
Co^{2+}	-3.31
Ca^{2+}	-2.90
Na^+	-6.26
K^+	-6.40

As it results from Table 2, the best composition sensor has very good values of the selectivity coefficients.

The pH function of the sensor was studied by using 10^{-2} M chromium (III) solutions, adjusted with HCl and NaOH to pH ranges varying from 1.5 to 11 and the obtained results are presented in Figure 6.

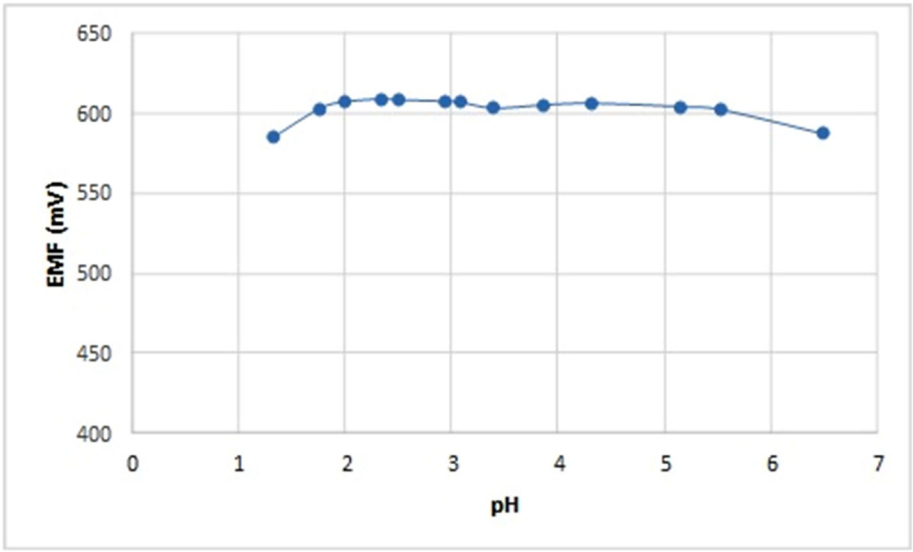

Figure 6. Effect of the pH of chromium(III) solution on the potentiometric answer.

As it results, the sensor has a useful pH range from 2.0 to 5.5. Above this pH value the precipitation of chromium(III) hydroxide is taking place.

The analytical usefulness of the sensor was tested in three different synthetic solutions by direct potentiometry with good results, as it can be seen in Table 3.

Table 3. Analytical application of the chromium(III)-sensor in synthetic samples

Sample	Chromium in solution (g/L)	Chromium found by the electrode (g/L)	Recovery (%)
A	0.026	0.024	92.3
B	0.26	0.25	96.2
C	1.30	1.313	101.0

CONCLUSIONS

The aggregation behavior and ion detection properties of 5-(4-pyridyl)-10,15,20-tris(phenoxy-phenyl)porphyrin were investigated.

TEM and STEM analyses revealed the formation of circular, elliptical and spherical aggregates. The circular and elliptical structures group together into collections of aggregates bearing ovoidal shapes, while the spherical ones can join together into bunches. Diameter measurements revealed some of those aggregates to be in the nanoscale.

Electron tomography was used to obtain the 3D representation of a porphyrin aggregate. Sections through this structure reveal its interior to be almost entirely filled.

A PVC membrane-based chromium(III)-selective electrode incorporating the porphyrin as ionophore was formulated and evaluated. The sensor exhibited a slope of 18.11 mV/decade over the chromium concentration range of $3x10^{-5} \div 10^{-1}$ M and it may be used in a pH range from 2.0 to 5.5 with very good values of the selectivity coefficients. With the aim of improving these results, future studies will focus on the use of gold nanoparticle-based microchip systems.

EXPERIMENTAL SECTION

Reagents. The synthesis, purification and characterization of the 5-(4-pyridyl)-10,15,20-tris(phenoxy-phenyl)porphyrin (Scheme 1) were previously published [29].

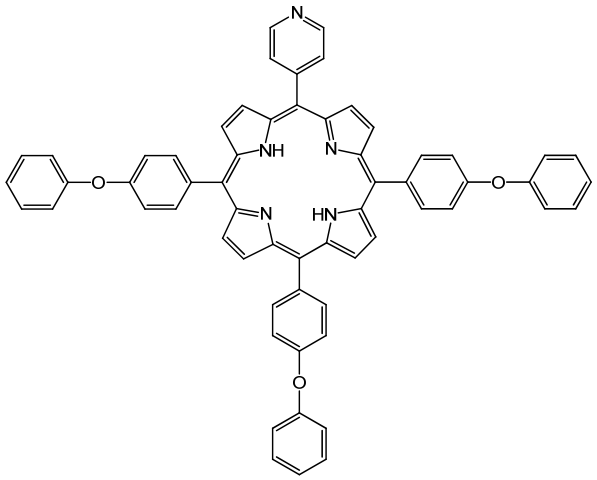

Scheme 1. *The structure of 5-(4-pyridyl)-10,15,20-tris(phenoxy-phenyl)porphyrin*

TEM samples were prepared using tetrahydrofurane (THF) purchased from Sigma Aldrich. PVC membranes incorporating the porphyrin ionophore were prepared using high molecular weight poly(vinyl)chloride, *o*-nitrophenyloctylether (NPOE), dioctylphtalate (DOP), bis(2-ethylhexyl)sebacate (DOS), sodium tetraphenylborate (NaTPB) and THF purchased from Fluka, Merck and Sigma Aldrich. All reagents (salts, acids and bases) were of analytical reagent grade. Double distilled water was used throughout the studies. The potentiometric response of each sensor was investigated in the $10^{-6} \div 10^{-1}$ M range of different cationic solutions. 0.1 M stock solutions were prepared by dissolving metal nitrates in double distilled water and standardized if necessary.

Preparation of TEM samples and analysis. The A_3B porphyrin was solubilized in THF and a solution of 0.15 mM was obtained. Drops of this solution were applied on TEM copper grids covered with continuous carbon film. The analysis was performed using a Titan G2 80-200 TEM/STEM microscope purchased from FEI Company in The Netherlands. The images were recorded in TEM and STEM modes at 80 and 200 kV acceleration voltages, using the software: Digital Micrograph v. 2.12.1579.0 and TEM Imaging & Analysis v. 4.7. The Electron Tomography tilt-series was obtained in STEM mode with the same microscope. Subsequent processing, including stack alignment and volume reconstruction, was performed using Inspect3D v. 4.0 software, while Avizo v. 9.0 was used for analyzing the 3D dataset.

Electrode membrane preparation and measurements. Three membranes having the composition: 1% ionophore, 33% PVC and 66% plasticizer were made. Sodium tetraphenylborate was used as additive (20 mol% relative to ionophore). Three different plasticizers: DOS, NPOE and DOP were used. One membrane was prepared in the composition 1,4% ionophore, 32,87% PVC and 65,73% plasticizer. Initially, the solvent mediator was mixed together with the porphyrin. Afterwards, the PVC with the appropriate amount of THF were added and mixed until a homogenous solution was obtained. This solution was transferred onto a glass plate and the THF was allowed to evaporate at room temperature until a tough and flexible membrane embedded in a PVC matrix was formed. Round shaped pieces of membranes (having diameters of 8 mm) were cut out and assembled on a Fluka electrode body. The measurements were performed at room temperature using a Hanna Instruments HI223 pH/mV-meter and the following cell setup:

Ag/AgCl/KCl (sat.) / sample solution / ion-selective membrane / conductive support (Cu) / internal cable

Prior to the potentiometric measurements, all membrane based sensors were conditioned for 24 h by soaking in 10^{-2} M Cr^{3+}. The detection limit of each sensor was established at the intersection point of the extrapolated linear mid-range and final low concentration level segments of the calibration plot. Potentiometric selectivity coefficients were determined according to the separate solution method [30] using equation (1) with a theoretical slope of 19.73 mV/decade of activity for chromium(III) cation and the potential values obtained for 10^{-2} M cation solutions.

$$\log K_{X,Y}^{pot} = \frac{(E_Y - E_X)\cdot z_X \cdot F}{RT\ln 10} + \left(1 - \frac{z_X}{z_Y}\right)\cdot \lg a_X \qquad (1)$$

The pH effect on the potentiometric response of the sensor was obtained by immersing the best chromium(III) sensor in solutions of NaOH and HCl in the 1.5 ÷ 11.0 pH range.

Analytical application. The best chromium(III) sensor was used for chromium detection in three synthetic solutions by direct potentiometry.

ACKNOWLEDGMENTS

The authors from the National Institute of Research-Development for Electrochemistry and Condensed Matter Timisoara kindly acknowledge Programme PN contract No. 09-34 02 07

R E F E R E N C E S

1. D.E. Kimbrough, Y. Cohen, A.M. Winer, L. Creelman, C.A. Mabuni, *Critical Reviews in Environmental Science and Technology*, **1999**, *29*, 1.
2. McGraw-Hill, "Concise Encyclopedia of Science and Technology", 5th edition, McGraw-Hill, New York, **2004**.
3. H.A. Zamani, M.R. Ganjali, M.R. Abedi, P. Norouzi, *Sensor Letters*, **2007**, *5*, 1.
4. R.K. Sharma, A. Goel, *Analytica Chimica Acta*, **2005**, *534*, 137.
5. Y. Masuda, E. Ishida, K. Hiraga, *Nippon Kagaku Kaishi*, **1980**, *10*, 1453.
6. S.S.M. Hassan, M.N. Abbas, G.A.E. Moustafa, *Talanta*, **1996**, *43*, 797.
7. A.K. Singh, A. Panwar, S. Kumar, S. Baniwal, *Analyst*, **1999**, *124*, 521.
8. A. Abbaspour, A. Izadyar, *Talanta*, **2001**, *53*, 1009.
9. T.V. Velikanova, A.N. Titov, M.A. Malkova, *Journal of Analytical Chemistry*, **2001**, *56*, 666.
10. M.B. Gholivand, F. Sharifpour, *Talanta*, **2003**, *60*, 707.
11. A. Sil, V. S. Ijeri, A.K. Srivastava, *Analytical and Bioanalytical Chemistry*, **2004**, *378*, 1666.
12. A.K. Singh, R. Singh, P. Saxena, *Sensors*, **2004***, 4*, 187.
13. M.R. Ganjali, P. Norouzi, F. Faridbod, M. Ghorbani, M. Adib, *Analytica Chimica Acta*, **2006**, *569*, 35.
14. V.K. Gupta, A.K. Jain, P. Kumar, S. Agarwal, G. Maheshwari, *Sensors and Actuators B*, **2006**, *113*, 182.
15. M. Kia, H. Aghaie, M. Arvand, K. Zare, M. Aghaie, *Journal of Physical & Theoretical Chemistry Islamic Azad University of Iran,* **2006**, *3*, 105.
16. H.A. Zamani, G. Rajabzadeh, M.R. Ganjali, *Sensors and Actuators B*, **2006**, *119*, 41.
17. H.A. Zamani, G. Rajabzadeh, M. Masrornia, A. Dejbord, M.R. Ganjali, N. Seifi, *Desalination*, **2009**, *249*, 560.
18. H.A. Zamani, S. Sahebnasagh, *International Journal of Electrochemical Science*, **2013**, *8*, 3708.
19. V.K. Gupta, A.K. Jain, Z. Ishtaiwi, H. Lang, G. Maheshwari, *Talanta*, **2007**, *73*, 803.
20. D. Vlascici, E. Fagadar-Cosma, I. Popa, V. Chiriac, M. Gil-Agusti, *Sensors*, **2012**, *12*, 8193.
21. D. Vlascici, I. Popa, V.A. Chiriac, G. Fagadar-Cosma, H. Popovici, E. Fagadar-Cosma, *Chemistry Central Journal*, **2013**, *7*, 111.
22. V. Snitka, M. Rackaitis, R. Rdaite, *Sensors and Actuators B,* **2005**, *109*, 159.
23. Q. Liu, Y. Yang, H. Li, R. Zhu, Q. Shao, S. Yang, J. Xu, *Biosensors and Bioelectronics*, **2015**, *64*, 147.
24. L. Yang, N. Larouche, R. Chenitz, G. Zhang, M. Lefevre, J.P. Dodelet, *Electrochimica Acta*, **2015**, *159*, 184.
25. P.A. Midgley, R. Dunin-Borkowski, *Nature Materials*, **2009**, *8*, 271.
26. G.S. Liu, S.D. House, J. Kacher, M. Tanaka, K. Higashida, I. M. Robertson, *Materials Characterization*, **2014**, *87*, 1.

27. T. Djuric, T. Ules, S. Gusenleitner, N. Kayunkid, H. Plank, G. Hlawacek, C. Teichert, M. Brinkmann, M. Ramsey, R. Resel, *Physical Chemistry Chemical Physics*, **2012**, *14*, 262.
28. H.H. Mezerji, W.V. den Broek, S. Bals, *Ultramicroscopy*, **2011**, *111*, 330.
29. E. Fagadar-Cosma, G. Fagadar-Cosma, M. Vasile, C. Enache, *Current Organic Chemistry*, **2012**, *16*, 931.
30. Y. Umezawa, P. Buhlmann, K. Umezawa, K. Tohda, *Pure and Applied Chemistry*, **2000**, *72*, 1851.